

Proposal for the direct optical detection of pure spin currents in semiconductors

Jiang-Tao Liu and Kai Chang*

SKLSM, Institute of Semiconductors, Chinese Academy of Sciences, P.O. Box 912, Beijing 100083, China

(Received 20 April 2008; published 3 September 2008)

We suggest a different practical scheme for the direct detection of pure spin current by using the two-color Faraday rotation of optical quantum interference process (QUIP) in a semiconductor system. We demonstrate theoretically that the Faraday rotation of QUIP depends sensitively on the spin orientation and wave vector of the carriers, and can be tuned by the relative phase and the polarization direction of the ω and 2ω laser beams. By adjusting these parameters, the magnitude and direction of the spin current can be detected.

DOI: [10.1103/PhysRevB.78.113304](https://doi.org/10.1103/PhysRevB.78.113304)

PACS number(s): 78.20.Ls, 42.65.-k, 72.25.Dc

Generating spin population in semiconductors is one of the central goals of spintronics and has attracted a rapidly growing interest for its potential application in spintronic devices. For pure spin current, the spin-up and spin-down electron currents are expected to have equal magnitudes but travel in opposite directions ($\pm\mathbf{k}$). In semiconductors, these currents can be generated by utilizing the spin Hall effect (SHE),¹⁻⁴ the optical quantum-mechanical interference control between one- and two-photon excitations,⁵⁻⁹ and the one-photon absorption in the noncentrosymmetric semiconductors.^{10,11} However, the experimental measurement of spin current is an extremely challenging task. The pure spin current can only be detected indirectly in semiconductors by measuring the spin accumulation^{4-7,12} near the boundary of the sample—the nonuniform spatial distribution, i.e., spin wavepacket.¹¹ So far, the direct measurement of a pure spin current, with *uniform* spatial spin and charge distributions, has still not been reported in semiconductor structures since the pure spin current exhibits vanishing charge current and total spin. The vanishing charge current and total spin make *direct* electrical or optical detections in semiconductor structures extremely difficult.

Is it possible to detect the uniform pure spin current in a semiconductor system? Although the total spin of a uniform pure spin current vanishes everywhere in the real space, the spin population is asymmetric in the momentum space, i.e., the asymmetric distribution of the spin-up (-down) electrons at opposite $\pm\mathbf{k}$ points. Direct optical detection would be possible if the optical transition at $\pm\mathbf{k}$ points become asymmetric by utilizing a quantum interference process (QUIP), e.g., the two-photon process. The momentum-resolved optical transition can be detected by circularly polarized light [Faraday rotation (FR) or Kerr rotation] and magnetic circular dichroism. In this work, we focus on the Faraday rotation spectrum because it is a powerful tool for investigating the spin dynamics of carriers in semiconductors.¹³ The conventional FR vanishes for the detection of pure spin current since it is determined by the total spin of the system, i.e., the difference of the spin-up and spin-down electron populations.

In this Brief Report, we suggest a different scheme by utilizing a momentum-resolved two-color FR of optical quantum interference process for direct detection of spin current in a semiconductor structure. In the quantum interference process between one- and two-photon absorptions, the transition rate depends, not only on the polarizations of the laser pulses, but also on the relative phase of the ω and 2ω

excitations, which makes the transition rate depend on electron wave vector \mathbf{k} . The optical transition of QUIP can be enhanced at $+\mathbf{k}$ but vanishes at $-\mathbf{k}$ or *vice versa*. Therefore, it is possible to transfer the angular momentum between the photon and the electron-hole pair at a specific \mathbf{k} point, while it is forbidden at the opposite $-\mathbf{k}$ point. Thus, the FR of QUIP can be used to detect the spin population at opposite $\pm\mathbf{k}$ points independently, i.e., the pure spin current case, by adjusting the external parameter such as the relative phase between the ω and 2ω excitations.

Supposing there is a pure spin current in semiconductor structures, we study the FR of a two-photon (ω and 2ω) quantum interference process. First, instead of perturbation theory, we calculate the transition rate for the one- and two-photon absorptions using the Wolkow-type wave function, which describes the electron state under an optical field of arbitrary intensity.¹⁴ Then, we give the analytical expression of the FR of QUIP in a three-dimensional (3D) sample. The valence and conduction states can be expressed as a Wolkow-type dressed state,

$$\psi_{c,v}(\mathbf{k}, \mathbf{r}, t) = u_{c,v}(\mathbf{k}, \mathbf{r}) \exp \left[i\mathbf{k} \cdot \mathbf{r} - i\omega_{c,v}t + \frac{ie}{m_{c,v}} \int_0^t \mathbf{k} \cdot \mathbf{A}(\tau) d\tau \right], \quad (1)$$

where c (v) refers to the conduction (valence) band, $u_{c,v}(\mathbf{k}, \mathbf{r})$ are the band-edge Bloch wave functions, $E_{c,v}(k) = \hbar\omega_{c,v}(k)$ is the energy of the valence or conduction bands, $m_{c,v}$ are the effective masses, and \mathbf{A} is the total vector potential $\mathbf{A} = \mathbf{a}_1 A_1 \cos(\omega t + \varphi_\omega) + \mathbf{a}_2 A_2 \cos(2\omega t + \varphi_{2\omega})$. $\mathbf{a}_1, A_1, \varphi_\omega$ ($\mathbf{a}_2, A_2, \varphi_{2\omega}$) are the polarization unit vector, the amplitude, and the phase of the ω (2ω) light, respectively. The excitation field satisfies the relation $\hbar\omega < E_g < \hbar 2\omega < E_g + \Delta_0$, where Δ_0 is the spin-orbit splitting, so that the ω and 2ω excitations generate independent carriers through two- and one-photon absorptions. The transition rate is calculated using an S -matrix formalism,¹⁴

$$S = -\frac{i}{\hbar} \int_{-\infty}^{\infty} dt \int d^3r \psi_c^*(\mathbf{k}, \mathbf{r}, t) H_{\text{int}} \psi_v(\mathbf{k}, \mathbf{r}, t). \quad (2)$$

The transition rate is

$$W(\mathbf{k}) = C \left\{ \left(\frac{\eta_1}{2} \right)^2 |\mathbf{P}_{cv} \cdot \mathbf{a}_1|^2 A_1^2 + |\mathbf{P}_{cv} \cdot \mathbf{a}_2|^2 A_2^2 + \left[A_1 A_2 \frac{\eta_1}{2} (\mathbf{P}_{cv} \cdot \mathbf{a}_1)^* (\mathbf{P}_{cv} \cdot \mathbf{a}_2) e^{i(2\varphi_\omega - \varphi_{2\omega})} + \text{c.c.} \right] \right\}, \quad (3)$$

where $C = 2\pi \left(\frac{e}{2\hbar m_0 c} \right) \delta[\omega_{cv}(k) - 2\omega] (f_v - f_c)$, f_v (f_c) is the Fermi function value of valence (conduction) electrons in \mathbf{k} , ω_{cv} is the optical transition frequency, $\mathbf{P}_{cv} = \langle c | \hat{p} | v \rangle$, $\eta_1 = \frac{eA_1}{\omega c m_{cv}} \mathbf{k} \cdot \mathbf{a}_1$, $1/m_{cv} = 1/m_c - 1/m_v$, and m_c (m_v) are the effective masses of electrons (holes). The term in the square brackets describes the quantum interference between the one- and two-photon excitations. From Eq. (3), the quantum interference term depends sensitively on the electron wave vector \mathbf{k} , the electron-spin orientation, the polarization, and the relative phase of the pulses. The transition rate can be strongly asymmetric for the transitions at $\pm \mathbf{k}$, e.g., $W(-\mathbf{k}) = 0$ while $W(+\mathbf{k}) \neq 0$ by adjusting the polarization and the relative phase of the pulses. The electron and hole states in Eq. (2) can be obtained from the single-band and the multi-band Luttinger-Kohn (LK) effective-mass Hamiltonians, respectively.¹⁵ The LK Hamiltonian reads

$$H_h(z_h, \rho) = \frac{\hbar^2 k^2}{2m_0} \begin{pmatrix} H_{hh} & L & M & 0 \\ L^* & H_{lh} & 0 & M \\ M^* & 0 & H_{lh} & -L \\ 0 & M^* & -L^* & H_{hh} \end{pmatrix}, \quad (4)$$

where

$$H_{hh} = -\gamma_1 - \gamma_2 (\sin^2 \theta_e - 2 \cos^2 \theta_e),$$

$$H_{lh} = -\gamma_1 + \gamma_2 (\sin^2 \theta_e - 2 \cos^2 \theta_e),$$

$$M = -\sqrt{3} \gamma_2 \sin^2 \theta_e e^{-2i\varphi_e},$$

$$L = i2\sqrt{3} \gamma_3 \sin \theta_e \cos \theta_e e^{-i\varphi_e},$$

where $\mathbf{k} = (k, \theta_e, \varphi_e)$ and γ_1 , γ_2 , and γ_3 are the Luttinger parameters. The energy dispersions of valence subbands in the isotropic approximation $\gamma_2 = \gamma_3$ are $E_{\pm} = \frac{\hbar^2 k^2}{2m_0} [-\gamma_1 \pm (R_h^2 + |L|^2 + |M|^2)^{1/2}]$ and $R_h = -\gamma_2 (\sin^2 \theta_e - 2 \cos^2 \theta_e)$. The eigenstate vectors of the heavy-hole (hh) and light-hole (lh) bands are $|hh_+\rangle = \frac{1}{c_h} (R_h + E'_+, L^*, M^*, 0)^T$, $|hh_-\rangle = \frac{1}{c_h} (0, M, -L, R_h + E'_+)^T$ and $|lh_+\rangle = \frac{1}{c_h} (L, -R_h + E'_-, 0, M^*)^T$, $|lh_-\rangle = \frac{1}{c_h} (M, 0, -R_h + E'_-, -L^*)^T$, respectively, where c_h is a normalization constant, (...) ^T denotes the transpose of a matrix, and $E'_{\pm} = \pm \sqrt{|M|^2 + |L|^2 + R_h^2}$ is the energy difference between the hh and lh bands.

As shown schematically in Fig. 1(a), the ω and 2ω two-color optical fields are linearly parallel polarized along the x axis and propagate along $+z$, $\mathcal{E}(\mathbf{r}, t) = \mathcal{E}_\omega e^{i(\omega t - \mathbf{k}_\omega \cdot \mathbf{r} + \varphi_\omega)} \hat{e}_\omega + \mathcal{E}_{2\omega} e^{i(2\omega t - \mathbf{k}_{2\omega} \cdot \mathbf{r} + \varphi_{2\omega})} \hat{e}_{2\omega}$, and \hat{e}_ω and $\hat{e}_{2\omega}$ are the unit polarization vectors. The propagation directions, \mathbf{k}_ω and $\mathbf{k}_{2\omega}$, are both along $+\hat{z}$. Using Eq. (3), the difference of the transition rate δW for the right- and left-circular-polarized lights in the presence of the pure spin current can be written as

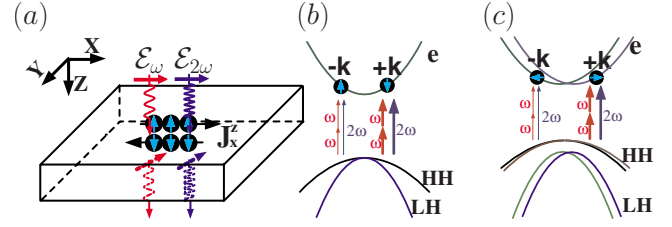


FIG. 1. (Color online) (a) Schematic of two parallel linearly polarized beams propagating in semiconductor structures in the presence of a uniform pure spin current. The band structure of a (b) 3D sample without the SOI and (c) 2D quantum well with the SOIs. The thickness of the red vertical arrows indicates the strength of the transitions of QUIP.

$$\begin{aligned} \delta W &= \sum_{\mathbf{k}} W_+(\mathbf{k}) + W_+(-\mathbf{k}) - W_-(\mathbf{k}) - W_-(-\mathbf{k}) \\ &= \sum_{\mathbf{k}} C_0 [C_{i1} (f_u + f_d) \cos(2\varphi_\omega - \varphi_{2\omega}) \\ &\quad + C_{i2} \sin(2\varphi_\omega - \varphi_{2\omega}) \sin(2\varphi_e) (f_d - f_u) \\ &\quad + C_i (f_u - f_d)] \delta[\omega_{cv}(k) - 2\omega], \end{aligned} \quad (5)$$

where

$$C_0 = 2\pi \frac{2}{\sqrt{2} c_h^2} \left(\frac{e}{\hbar 2m_0 c} \right)^2 P^2,$$

$$C_{i1} = \frac{\eta_1}{2} A_1 A_2 k \sin \theta_e \cos \varphi_e \mathfrak{R}_{h,l},$$

$$C_{i2} = \frac{\eta_1}{2} A_1 A_2 k \sin \theta_e \cos \varphi_e \mathfrak{I}_{l,h} \text{Re}(M) / \sqrt{3},$$

$$C_i = A_2^2 \mathfrak{R}_{h,l},$$

where $\mathfrak{R}_h = [(R_h + E'_+)^2 - (|M|^2 + |L|^2)/3]$ and $\mathfrak{I}_h = 2(R_h + E'_+)$ denote the contributions from the transition from the hh band to the conduction band, and $\mathfrak{R}_l = [|M|^2 + |L|^2 + (R_l - E'_-)^2 / 3]$ and $\mathfrak{I}_l = 2(E'_- - R_l)$ for the transition from the lh band to the conduction band. $W_+(\pm \mathbf{k})$ ($W_-(\pm \mathbf{k})$) denotes the transition rate for the left- (right-) circular-polarized 2ω optical field and linear-polarized ω optical field at $\pm \mathbf{k}$, and f_u (f_d) is the occupation number of spin-up (spin-down) electrons in the conduction band at $+\mathbf{k}$ ($-\mathbf{k}$), $P^2 = |\langle S | P_x | X \rangle|^2$, where $|S\rangle$, $|X\rangle$, $|Y\rangle$, and $|Z\rangle$ denote the Kohn-Luttinger amplitudes, $\eta_1 = \frac{eA_1}{\omega c m_{cv}}$. The difference of the refractive index for the right- and left-circular-polarized lights is $\delta\alpha = n\hbar\omega\delta W / c_0 \mathcal{U}$, where c_0 is the speed of light, n is the refractive index, and \mathcal{U} is the energy density. The real part of dielectric constant can be obtained by using the Kramers-Kronig relationship. Thus, the FR angle of the 2ω pulse per unit length is given by $\theta_F(\omega) = \frac{\omega}{c} \text{Re}(N_+ - N_-)$,¹⁶ where N_+ (N_-) is the refractive index for the left- (right-) circular-polarized lights.

The first two terms in Eq. (5) represent the FR of QUIP arising from the quantum interference between one- and two-photon absorptions. The interference terms are linearly proportional to the wave vector \mathbf{k} [see Eq. (3)] and, consequently, FR is proportional to the spin current density $\mathbf{J}_s^z = \frac{1}{2} \langle \sigma_z \mathbf{v}_i + \mathbf{v}_i \sigma_z \rangle \sim \sum_{\mathbf{k}} [f_u(\mathbf{k}) + f_d(-\mathbf{k})] \mathbf{k}$, $i, j = x, y, z$. Therefore, the FR of QUIP can detect the spin current directly. The third

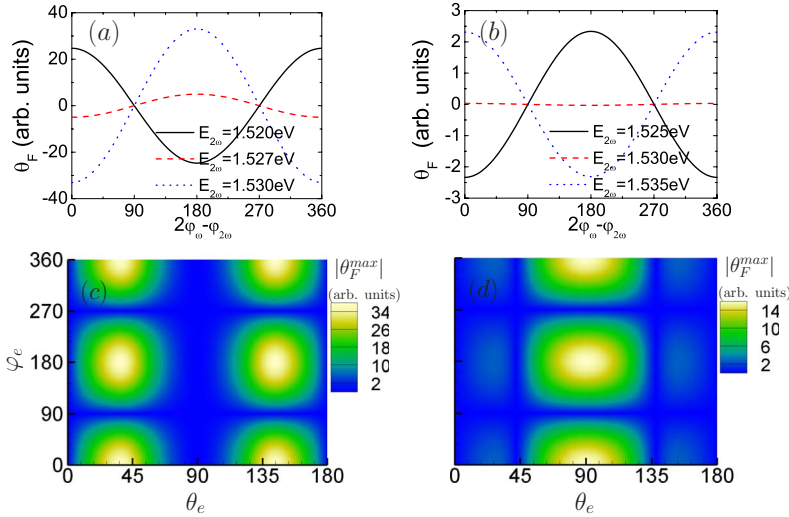


FIG. 2. (Color online) FR of QUIP (θ_F) as a function of the relative phase of the lights for (a) the hh -conduction-band and (b) the lh -conduction-band transition processes, $\theta_e = 30^\circ$. (c) and (d) show the contour plot of the QUIP FR ($|\theta_F^{max}|$) as a function of polar angles θ_e and φ_e of electron wave vector for the hh -conduction-band and the lh -conduction-band transition processes at $2\varphi_\omega - \varphi_{2\omega} = 0^\circ$, respectively.

term in Eq. (5) is the single-photon transition term corresponding to the conventional FR, which is independent of the electron wave vector \mathbf{k} . For the pure spin current, i.e., $f_{u}(\mathbf{k}) = f_{d}(-\mathbf{k})$, the conventional FR vanishes since the total spin of the pure spin current vanishes. Thus, the conventional FR cannot detect the spin current directly if we neglect the negligible small wave vector of light. The transition rates of two- and one-photon absorptions can be set equal by tuning the intensity of laser beams, i.e., $\eta_1 A_1/2 \approx A_2$. The FR of QUIP in the detection of pure spin current is of the same order as the conventional FR.

In order to detect the pure spin current $J_j^i (i, j = x, y, z)$ in semiconductor structures, the magnitude and direction of electron velocity and the electron-spin orientation are necessary. Figures 2(a) and 2(b) show the FR of QUIP as a function of the relative phase between the ω and 2ω optical fields in the presence of a pure spin current in bulk GaAs material.¹⁷ To ensure phase matching between ω and 2ω optical excitations, the thickness of the sample should be less than the coherence length l_{coh} .²¹ The FR of QUIP reaches its maxima at $2\varphi_\omega - \varphi_{2\omega} = 0^\circ, 180^\circ$, and 360° and vanishes at $2\varphi_\omega - \varphi_{2\omega} = 90^\circ$ and 270° . One can determine the spin-up and spin-down electron populations $f_{u,d}$ at a specific wave vector \mathbf{k} by setting the different phase differences $2\varphi_\omega - \varphi_{2\omega}$ [see Eq. (5)]. The FR of QUIP can also be used to determine the direction of the spin current and the polarization of the laser pulse [see the $\eta_1 \sim \mathbf{k} \cdot \mathbf{a}_1$ term in Eq. (3)], e.g., the FR of QUIP vanishes at $\varphi_e = 90^\circ$ or $\theta_e = 0^\circ$. Figures 2(c) and 2(d) describe the maximum of the FR of QUIP as a function of the direction of the electron wave vector, i.e., polar angles θ_e and φ_e for $2\varphi_\omega - \varphi_{2\omega} = 0^\circ$. Utilizing the relationship between the FR of QUIP and the direction of the electron wave vector, the direction of the spin current can be determined experimentally. The oscillating FR of QUIP arises from the interplay between the propagation direction of the light and the direction of the electron wave vector, and the mixing of heavy-hole and light-hole states [see Eq. (5) and $\mathfrak{R}_{h,l}$]. The hole mixing effect shortens the oscillation period of the FR of QUIP from 2π to π .

Comparing the left panel with the right panel of Fig. 2, the contribution to the FR of QUIP from the $hh_{\pm-c}$ band

transition is different from that from the $lh_{\pm-c}$ band transition due to the distinct energy dispersions and the Bloch band-edge wave functions. The distinct energy dispersions make the optical transition occur at different wave vectors for the hh and $lh-c$ band transitions, while the Bloch band-edge wave functions of the hh and lh bands determine the strengths of the corresponding transitions, i.e., the magnitude of the FR of QUIP.

Now we turn to discuss the detection of pure spin current in the two-dimensional (2D) GaAs quantum well (QW) (Ref. 17) in the presence of the spin-orbit interactions (SOIs) [see Fig. 1(c)], i.e., Dresselhaus SOI and Rashba SOI.^{18–20} The difference between the 3D and 2D samples is the lifted degeneracy of the hh and lh bands at Γ point and the spin degeneracy caused by the SOIs. We can detect the spin orientation and direction of the pure spin current in the two-dimensional case. Likewise, the FR of QUIP also vanishes when the polarization vector \mathbf{a}_1 is perpendicular to the direction of the pure spin current. Figure 3(a) depicts the FR of QUIP as a function of the direction of the electron wave vector φ_e for an out-of-plane-oriented spin current $J_{\varphi_e}^z$. As in 3D sample, the relative phase can also be used to tune the FR of QUIP [see Fig. 3(b)], which shows a cosine function with the relative phase. Figures 3(c) and 3(d) show the FR of QUIP as a function of the electron-spin orientation and the propagation direction of the laser pulse. When the spin orientation is along the z axis, the FR of QUIP from the $hh-c$ band transition increases since the $|X\rangle$ component of the hh band is crucial for the FR of QUIP. A strongly anisotropic FR can be found in Fig. 3(d) as a function of the propagation direction of laser pulses and the spin orientation $\langle \sigma_z \rangle$, which is caused by the anisotropic transition matrix elements $\langle c|\mathbf{p}|v\rangle \sim -\frac{1}{6}\langle S|\cos\theta_{p_x}|X\rangle + \frac{\sqrt{2}}{3}\langle S|\sin\theta_{p_z}|Z\rangle$. Thus, we can obtain information about the spin orientation of spin currents by altering the propagation direction of laser pulses. We find that the transition between the $lh-c$ bands leads to a larger FR than that of the $hh-c$ transition since the FR of QUIP for in-plane-oriented spin current is dominantly determined by the $|Z\rangle$ component in the hole states. The $|Z\rangle$ component in the band-edge Bloch wave function of the light-hole band $|lh\rangle = (1/\sqrt{6})[|X\rangle \pm i|Y\rangle \otimes |\downarrow\uparrow\rangle - 2|Z\rangle \otimes |\uparrow\downarrow\rangle]$ is stronger than

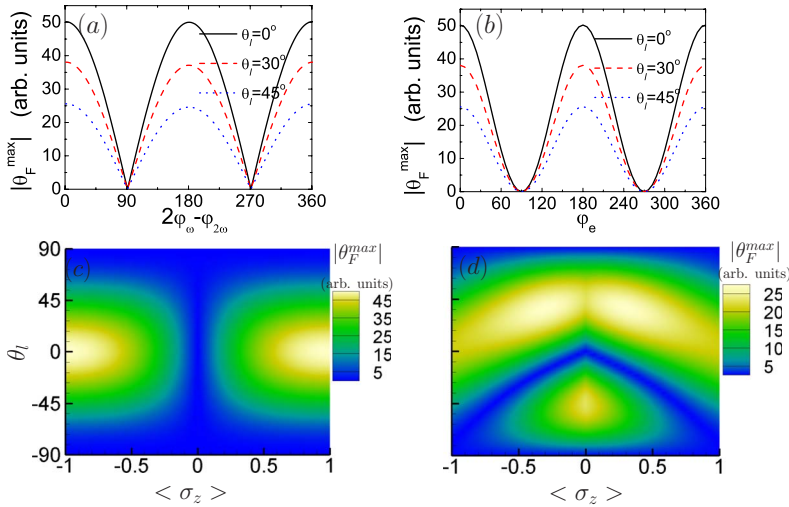


FIG. 3. (Color online) (a) FR of QUIP as a function of the relative phase and (b) the direction of electron wave vector for the hh - c band transition process. θ_l denotes the different propagation directions of pulses. (c) and (d) show the contour plot of the QUIP FR as functions of the spin-polarization direction and propagation direction of pulses for the hh - c band and lh - c band transition processes, respectively.

that in the heavy-hole band $|hh\rangle = (1/\sqrt{2})(|X\rangle \pm i|Y\rangle) \otimes |\uparrow\downarrow\rangle$ in which the $|Z\rangle$ component primarily comes from the hole mixing effect, which is strong for large wave vectors.

Finally, we can also estimate the magnitude of FR of QUIP in realistic semiconductor systems. For the optical quantum interference injection⁶ in GaAs QWs, the carrier density is about 10^{17} cm^{-3} and the corresponding FR of QUIP from our calculations is about $20 \text{ mrad}/\mu\text{m}$. In a recent experiment,²² the spin Hall conductivity is about $3 \Omega^{-1} \text{ m}^{-1}/|e|$ at the electric field $E=36.2 \text{ mV}/\mu\text{m}$, the corresponding spin-up (spin-down) electron density is about 10^{13} cm^{-3} , and the FR of QUIP for this case is about $2 \mu\text{rad}/\mu\text{m}$, which is not difficult to detect using the current FR technique. The ultrafast lasers can control a quantum system on the femtosecond time scale, which is shorter than the electron-spin lifetimes and electron momentum relaxation times (about 0.19 – 1.2 ps),²³ especially in the n -type

layers, a long spin lifetime (10^3 – 10^4 ps) can be achieved.^{4,24}

In summary, we have suggested a different momentum-resolved scheme for the direct optical detection of a uniform pure spin current by utilizing the two-color FR of QUIP in bulk semiconductors and two-dimensional semiconductor quantum-well structures. By adjusting the incident angle, the polarization direction, the energy, and the relative phase between the ω and 2ω laser pulses, detailed information about the spin current can be detected directly. This scheme may also be important for distinguishing the extrinsic SHE and intrinsic SHE from the different dependence of the pure spin current on the crystal orientation. Our scheme can also be used to detect the spin polarization of the charge current.

This work was supported by the NSFC under Grant No. 60525405 and the knowledge innovation project of CAS. K.C. would like to acknowledge R. B. Liu for his discussions.

*Corresponding author. kchang@red.semi.ac.cn

¹M. I. D'yakov and V. I. Perel', Phys. Lett. **35A**, 459 (1971); J. E. Hirsch, Phys. Rev. Lett. **83**, 1834 (1999).

²S. Murakami, N. Nagaosa, and S. C. Zhang, Science **301**, 1348 (2003).

³J. Sinova *et al.*, Phys. Rev. Lett. **92**, 126603 (2004).

⁴Y. K. Kato, R. C. Myers, A. C. Gossard, and D. D. Awschalom, Science **306**, 1910 (2004).

⁵R. D. R. Bhat and J. E. Sipe, Phys. Rev. Lett. **85**, 5432 (2000).

⁶M. J. Stevens *et al.*, Phys. Rev. Lett. **90**, 136603 (2003).

⁷J. Hübner *et al.*, Phys. Rev. Lett. **90**, 216601 (2003).

⁸A. Haché *et al.*, Phys. Rev. Lett. **78**, 306 (1997).

⁹W. Yao, A. H. MacDonald, and Q. Niu, Phys. Rev. Lett. **99**, 047401 (2007).

¹⁰R. D. R. Bhat, F. Nastos, A. Najmaie, and J. E. Sipe, Phys. Rev. Lett. **94**, 096603 (2005).

¹¹H. Zhao *et al.*, Phys. Rev. B **72**, 201302(R) (2005).

¹²J. Wunderlich, B. Kaestner, J. Sinova, and T. Jungwirth, Phys. Rev. Lett. **94**, 047204 (2005).

¹³J. M. Kikkawa and D. D. Awschalom, Science **287**, 473 (2000).

¹⁴D. M. Wolkow, Z. Phys. **94**, 250 (1935); H. D. Jones and H. R. Reiss, Phys. Rev. B **16**, 2466 (1977); M. Sheik-Bahae, *ibid.* **60**, R11257 (1999).

¹⁵J. M. Luttinger, Phys. Rev. **102**, 1030 (1956).

¹⁶K. Shinagawa, in *Magneto-Optics*, edited by S. Sugano and N. Kojima (Springer-Verlag, Berlin, 1999).

¹⁷The following parameters of GaAs are used in our numerical calculation: $m_e=0.0665m_0$ (m_0 is the free electron mass), $\gamma_1=6.85$, $\gamma_2=2.1$, and the band gap $E_g=1.52 \text{ eV}$. The band-gap mismatch between GaAs and $\text{Al}_x\text{Ga}_{1-x}\text{As}$ $\Delta E_g=1.155x+0.37x^2$, $x=0.35$, $\Delta E_c/\Delta E_v=60/40$, Dresselhaus SOI and Rashba SOI parameters are taken from Refs. 18–20, $E_z=60 \text{ kV/cm}$, $\langle\alpha E_z\rangle=1 \text{ meV nm}$, $\langle\beta E_z\rangle=7.5 \text{ meV nm}$, $\alpha_c^*=35 \text{ eV \AA}^3$, $\alpha_v=-39 \text{ eV \AA}^3$, $\delta\alpha_v=-35 \text{ eV \AA}^3$.

¹⁸E. I. Rashba and E. Ya. Sherman, Phys. Lett. A **129**, 175 (1988).

¹⁹M. G. Pala, M. Governale, J. König, U. Zülicke, and G. Iannaccone, Phys. Rev. B **69**, 045304 (2004).

²⁰W. Yang and K. Chang, Phys. Rev. B **74**, 193314 (2006).

²¹J. M. Fraser and H. M. van Driel, Phys. Rev. B **68**, 085208 (2003).

²²N. P. Stern *et al.*, Phys. Rev. Lett. **97**, 126603 (2006).

²³J. L. Oudar *et al.*, Phys. Rev. Lett. **53**, 384 (1984); H. Zhao, A. L. Smirl, and H. M. van Driel, Phys. Rev. B **75**, 075305 (2007).

²⁴J. M. Kikkawa and D. D. Awschalom, Phys. Rev. Lett. **80**, 4313 (1998).